

## PRESENT STATUS OF THE LASER CHARGE EXCHANGE TEST USING THE 3-MeV LINAC IN J-PARC

H. Takei<sup>†</sup>, E. Chishiro, K. Hirano, Y. Kondo, S.I. Meigo, A. Miura, T. Morishita, H. Oguri, K. Tsutsumi, J-PARC Center, Japan Atomic Energy Agency, Tokai, Ibaraki, JAPAN

### Abstract

The Accelerator-driven System (ADS) is one of the candidates for transmuting long-lived nuclides, such as minor actinide (MA), produced by nuclear reactors. For efficient transmutation of the MA, a precise prediction of neutronics of ADS is required. In order to obtain the neutronics data for the ADS, the Japan Proton Accelerator Research Complex (J-PARC) has a plan to build the Transmutation Physics Experimental Facility (TEF-P), in which a 400-MeV negative proton ( $H^-$ ) beam will be delivered from the J-PARC linac. Since the TEF-P requires a stable proton beam with a power of less than 10 W, a stable and meticulous beam extraction method is required to extract a small amount of the proton beam from the high power beam using 250 kW. To fulfil this requirement, the Laser Charge Exchange (LCE) method has been developed. The LCE strips the electron of the  $H^-$  beam and neutral protons will separate at the bending magnet in the proton beam transport. To demonstrate the charge exchange of the  $H^-$ , a preliminary LCE experiment was conducted using a linac with energy of 3 MeV in J-PARC. As a result of the experiment, a charge-exchanged  $H^+$  beam with a power of about 5 W equivalent was obtained under the J-PARC linac beam condition, and this value almost satisfied the power requirement of the proton beam for the TEF-P.

### INTRODUCTION

The Accelerator-driven System (ADS) is one of candidates for transmuting long-lived nuclides such as minor actinide (MA) produced by nuclear reactors [1]. For the efficient transmutation of MA, precise prediction of the neutronic performance of ADS is required. In order to obtain the neutronics data for the ADS, the Japan Proton Accelerator Research Complex (J-PARC) has a plan to build the Transmutation Physics Experimental Facility (TEF-P) [2]. The critical assembly installed in the TEF-P, which is a small and low power reactor, operates below 500 W to prevent excessive radio-activation. To perform the experiments at the TEF-P with such reactor power, with an effective neutron multiplication factor ( $k_{eff}$ ) of around 0.97, the incident proton beam power must be less than 10 W. Because the J-PARC accelerators focus on much higher beam power, a low power proton beam extraction device of high reliability is indispensable.

The development of a laser charge exchange (LCE) technique for extraction of the low power proton beam from the high power proton beam is now underway. The LCE technique was originally developed to measure the proton beam profile [3]. To apply the LCE technique to

the beam separation device for the TEF-P, it is important to evaluate the efficiency of conversion to the low power proton beam and the long-term power stability of the low power proton beam in order to keep the thermal power of the assembly constant. Thus, a preliminary LCE experiment to measure the power of the low power proton beam was conducted using a linac with energy of 3 MeV in J-PARC. In this paper, the preliminary results of the LCE experiment are presented.

### LASER CHARGE EXCHANGE

Figure 1 illustrates the concept of the LCE device for the TEF-P [4]. When a laser beam is injected into a negative proton ( $H^-$ ) beam with energy of 400 MeV from the J-PARC linac, the charge of the  $H^-$  beam crossed with the laser beam becomes neutral ( $H^0$ ). Since the outer electron of the  $H^-$  is very weakly bound to the atom, it can easily be stripped by a laser light in the wavelength range of 800~1100 nm as shown in Fig.2 [5]. These  $H^0$  protons do not sense the magnetic field of a bending magnet, and are completely separated from the remaining  $H^-$  beam at the exit of the bending magnet. However, it is well-known that pre-neutralized  $H^0$  particles are produced by collision with the remaining gas in accelerator tubes and are transported with the main proton beam. When we apply the LCE technique to the  $H^-$  beam with the pre-neutralized protons, it becomes impossible to predict the total power of the extracted beam.

To eliminate the pre-neutralized protons, we were trying to perform laser injection and beam bending simultaneously in one magnet. When the laser is injected in the magnetic field of the bending magnet, the pre-neutralized proton goes straight along the beam inlet direction and can be separated from the clean low power proton beam at the exit of the bending magnet. The charge-exchanged  $H^0$  beam reaches the stripping foil. After passing the stripping foil, the  $H^0$  beam is converted to a positive proton ( $H^+$ ) beam and then delivered to the TEF-P target. A material with a low melting temperature will be used as the stripping foil to avoid high power beam injection to the TEF-P target. Hereafter, the low power  $H^+$  beam extracted from the high power  $H^-$  beam by using this LCE strategy is referred to as "the stripped  $H^+$  beam."

Figure 2 shows the photoneutralization cross-section of  $H^-$  ions as a function of photon wavelength in the centre-of-mass frame. We chose a fundamental wavelength of 1064 nm from the commercial Nd:YAG laser because this wavelength is near the peak of the photoneutralization cross-section of  $H^-$  ions. Even taking the Lorentz contraction effect into consideration, the photoneutralization cross-section for the  $H^-$  beam with energy of 400 MeV using the fundamental wavelength of Nd:YAG laser is

<sup>†</sup> takei.hayanori@jaea.go.jp

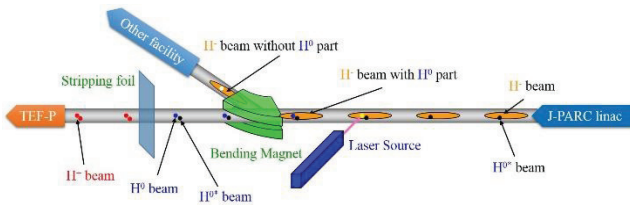


Figure 1: Conceptual diagram of the LCE device for TEF-P. The neutralized proton due to interaction by the laser light is written as “H<sup>0+</sup>”, and the pre-neutralized proton due to interaction by the remaining gas in accelerator tubes is written as “H<sup>0\*</sup>”.

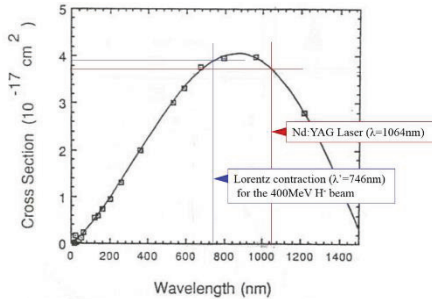


Figure 2: Cross section for H<sup>-</sup> photoneutralization as a function of photon wavelength in the centre-of-mass frame. The blue line shows the Lorentz contraction for the H<sup>-</sup> beam with 400 MeV.

Table 1: Specifications of the H<sup>-</sup> beam for the J-PARC linac and the 3-MeV linac

	J-PARC linac	3-MeV linac
Energy (MeV)	400	3
Maximum beam current (A)	$5.0 \times 10^{-2}$	$3.0 \times 10^{-2}$
Macropulse length (s)	$5.0 \times 10^{-4}$	$2.0 \times 10^{-4}$
Repetition rate (Hz)	25	25
Maximum beam power (W)	$2.5 \times 10^5$	$4.5 \times 10^2$
RF Frequency (MHz)	324	324
Beam power for a micro-bunch (W)	1.57	$6.95 \times 10^{-3}$

almost the same as that for the stationary H<sup>-</sup> ions using 1064 nm laser light. On the other hand, the Lorentz contraction effect of the collision with the 3-MeV H<sup>-</sup> beam and the 1064 nm laser light is insignificant. It is possible to experimentally estimate the conversion efficiency of the LCE for the TEF-P from the results of the LCE experiment with the 3-MeV linac.

Table 1 describes the specifications of the H<sup>-</sup> beam for the J-PARC linac and the 3-MeV linac. Here, the 3-MeV linac has two operational modes. Specifications for one of these two modes, *i.e.* the LCE experiment mode, are represented in this table. Based on theoretical considerations [4], the outer electrons of the H<sup>-</sup> ions can be stripped with an efficiency of almost 100% by using a commercial Nd:YAG laser having a pulse power of a few joules. Therefore, it is expected that a stripped H<sup>+</sup> beam with a power of 1.57 W can be obtained from a microbunch of the H<sup>-</sup> beam delivered from the J-PARC linac.

## LCE EXPERIMENT

### Experimental Devices

At J-PARC, a linac with energy of 3 MeV has been constructed for the development of accelerator components such as beam scrapers, bunch shape monitors, laser profile monitors, and so on. This linac consists of an H<sup>-</sup> ion source, a low energy beam transport, a radio frequency quadrupole (RFQ) linac, a medium frequency beam transport, and beam dumps. For further details about these devices, see ref. [6]. Hereafter, the linac with energy of 3 MeV is referred to as "the RFQ linac."

As shown in Figs. 3 and 4, the proton beam line consists of three quadrupole magnets which have a steering

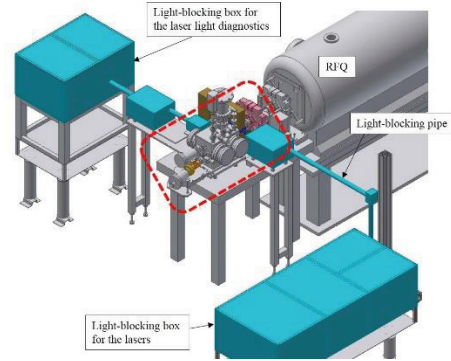


Figure 3: Layout of the RFQ linac with the laser system. The laser system are painted with light blue. Enlargement portion surrounded by the red dotted rectangle is shown in Fig.4.

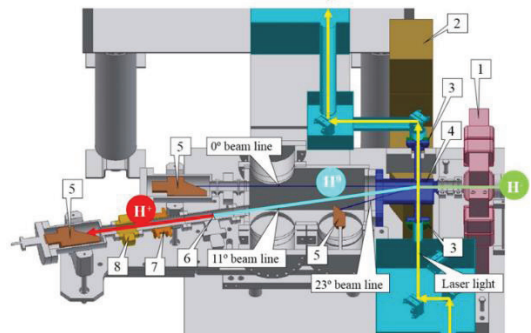


Figure 4: Schematic View of the LCE devices (1- quadrupole magnet, 2- bending magnet, 3- quartz viewing port, 4- vacuum chamber, 5- beam dump, 6- stripping foil, 7- BPM, 8- SCT).

Table 2: Specifications of the Nd:YAG laser and the He-Ne laser

	Nd:YAG laser	He-Ne laser
Operation mode	Pulsed	Continuous Wave
Wavelength (m)	$1.064 \times 10^{-6}$	$6.328 \times 10^{-7}$
Pulse width (s)	$(5 \sim 9) \times 10^{-9}$	—
Pulse energy (J)	1.6	—
Pulse repetition rate (Hz)	25	—
Power (W)	40	$2.0 \times 10^{-2}$

function, a bending magnet, a beam position monitor (BPM), beam current monitors, and beam dumps. The LCE devices were installed at the end of the proton beam line. That is, the titanium vacuum chamber was located between two magnetic poles of the bending magnet, in which the  $H^-$  beam collided with the Nd:YAG laser light at a near right angle. Two quartz viewing ports were fitted to the vacuum chamber. The commercial high power Q-switched Nd:YAG laser was located on an anti-vibration table. Table 2 describes the specifications of the Nd:YAG laser. The laser light was reflected by ten plane mirrors and transmitted through one quartz viewing port from the laser main body to the collision point. This optical path length was 4.25 m. After the collision with the  $H^-$  beam, the laser light was propagated to the termination point in the light-blocking box used for the laser light diagnostics. During the propagation, which was 3.16 m in length, there were five reflections by the plane mirror and one transmission through the quartz viewing port.

In this light-blocking box, three types of diagnostics for the Nd:YAG laser light were located. The first was a laser power meter (Gentec-EO, UP55N-50S-VR) to measure and absorb the laser light, the second was a photon beam profiler (Gentec, Beamage 4M) to measure the profile and the position of the laser light, and the third was a biplanar phototube (Hamamatsu Photonics K.K., R12290U-51) to measure the time structure of the laser light.

To keep the  $H^+$  beam power constant over longer periods, it was important to keep the position of the Nd:YAG laser light at the collision point constant. However, it was difficult to adjust the position of the invisible laser pulse of the Nd:YAG laser. Therefore, the visible laser light from the commercial He-Ne laser was used as a guide beam. The specifications of the He-Ne laser are also described in Table 2.

The trajectory of the  $H^-$  beam from the RFQ was bent by the bending magnet with a deflection angle of  $23^\circ$ , and transported to the beam dump provided in the most downstream part of the  $23^\circ$  beam line. As the Nd:YAG laser light was injected in the centre of the magnetic pole of the bending magnet, the  $H^0$  beam was transported to the beam line with the deflection angle of  $11.5^\circ$  and introduced to the stripping foil. Hereafter, this beam line is referred to as "the  $11^\circ$  beam line." The  $H^0$  beam was converted to the  $H^+$  beam by passing the stripping foil (cobalt-base alloy foil, Haver). From the upstream to the downstream of the  $11^\circ$  beam line, a BPM, a slow current transformer (SCT), and a Faraday cup (FC) serving as a beam dump were positioned.

### Experimental Method

At the end of June 2016, a preliminary LCE experiment to measure the power of the stripped  $H^+$  beam was conducted using the  $H^-$  beam derived from the RFQ linac.

First, the position of the  $H^-$  beam was measured by the BPM without exciting the bending magnet, and the trajectory of the  $H^-$  beam was adjusted by using steering magnets so that the  $H^-$  beam was passed through the centre position of the BPM. Beam width and emittance of the  $H^-$

beam were obtained with the beam emittance monitor placed 0.3 m downstream of the quadrupole magnet by using Q scan technique. As a result of the measurement, the root-mean-square (RMS) width in the vertical direction ( $\sigma_y$ ) at the collision point was estimated as about 2.8 mm.

After exciting the bending magnet, the  $H^-$  beam was transported to the  $23^\circ$  beam dump and collided with the Nd:YAG laser light. Then, the deflection angle of the  $H^-$  beam was decided by fine-tuning the magnetic field strength of the bending magnet so that the stripped  $H^+$  beam was passed through the centre position of the BPM located in the  $11^\circ$  beam line. By using beam current monitors such as SCT and FC, the current amount of the stripped  $H^+$  beam was measured.

Figure 5 shows the photon profile for the Nd:YAG laser observed by the photon beam profilers. From this figure, it can be seen that the RMS-radius of the Nd:YAG laser light was 3 mm at the exit of the laser main body and 4.7 mm at the termination point. The RMS-radius of the Nd:YAG laser light could be estimated as 3.9 mm at the collision point with the  $H^-$  beam if the spread of the Nd:YAG laser light was assumed to be increased in proportion to the optical path length. Therefore, from the viewpoint of the vertical direction for the  $H^-$  beam, the narrow  $H^-$  beam collided with the wide Nd:YAG laser light.

In addition, the Nd:YAG laser power was set to half of the rated output power (20 W, 0.8 J/pulse) to protect the quartz viewing port. The power of the Nd:YAG laser light gradually decreased until it reached the termination point due to the reflection by 15 plane mirrors and the transmission through two quartz viewing ports, and the laser power at the termination point was 14.7 W. Consequently, the total transmittance was estimated as 74%.

Figure 6 shows the time structure of the Nd:YAG laser light as a function of the laser power. Here, the values shown in the upper right corner of this figure are the laser powers at the termination point. The time profile of the

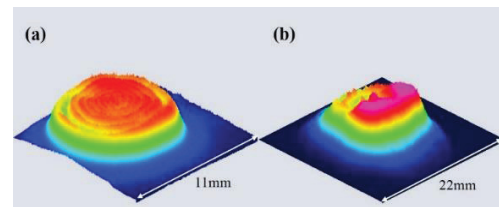


Figure 5: Three-dimensional photon profile for the Nd:YAG laser at (a) the exit of the laser main body and (b) the termination point.

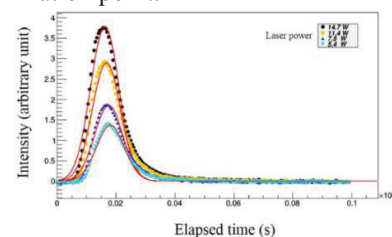


Figure 6: Time structure of the Nd:YAG laser light as a function of the laser power at the termination point.

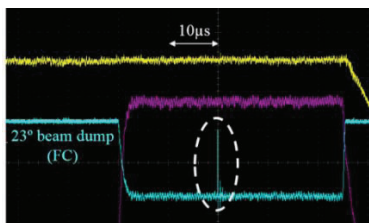


Figure 7: Current waveform of the H<sup>-</sup> beam observed at the 23° beam dump.

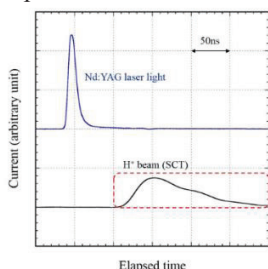


Figure 8: Waveform of the Nd:YAG laser pulse and the H<sup>+</sup> beam observed at the SCT of the 11° beam line.

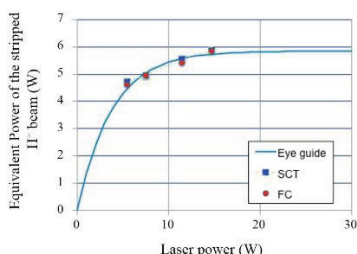


Figure 9: H<sup>+</sup> beam power as a function of the Nd:YAG laser power at the termination point.

Nd:YAG laser light with a power of 14.7 W had the pulse width of 4.8 ns ( $1\sigma$ ), and the time profile was independent of the laser power. From the time profile of the laser, it was obvious that a pulse of the Nd:YAG laser light collided with the 4.98 microbunches of the H<sup>-</sup> beam. Therefore, a stripped H<sup>+</sup> beam with a power of 7.5 W equivalent could be obtained under the assumption that the conversion efficiency for the horizontal direction of the H<sup>-</sup> beam was 100%.

### Preliminary Results

The light-blue broken line in Fig. 7 represents the current waveform of the H<sup>-</sup> beam observed at the 23° beam dump. This light-blue current waveform represents a single macropulse, and the rapid rise and fall part surrounded by the white dotted circle is due to the lack of the H<sup>-</sup> beam caused by the LCE. This lack was observed from the first shot of the Nd:YAG laser light after beginning the LCE experiment, and then we confirmed the collision between the H<sup>-</sup> beam and the Nd:YAG laser light. Figure 8 shows the pulse waveform of the Nd:YAG laser light observed at the biplanar phototube and the H<sup>+</sup> beam observed at the SCT of the 11° beam line. From the figure, it can be seen that the pulse waveform of the H<sup>+</sup> beam was obtained after the laser light, and the power of the H<sup>+</sup> beam was 0.026 W from the time integral of the H<sup>+</sup> beam current inside the dotted-red rectangle. If the laser light

from this Nd:YAG laser system collided with the H<sup>-</sup> beam delivered from the J-PARC linac, a stripped H<sup>+</sup> beam with a power of about 5 W would be obtained from the following equation.

$$0.026(\text{W}) \times \frac{400(\text{MeV})}{3(\text{MeV})} \times \frac{50(\text{mA})}{30(\text{mA})} = 5.7(\text{W}) \quad (1)$$

This value almost satisfied the power requirement (less than 10 W) of the proton beam for the TEF-P.

Figure 9 shows the equivalent power of the stripped H<sup>+</sup> beam under the J-PARC linac beam condition as a function of the Nd:YAG laser power. Here, the powers of the stripped H<sup>+</sup> beam were obtained using the SCT and FC. We confirmed that the equivalent powers of the stripped H<sup>+</sup> beam measured by using the SCT and FC were in good agreement, and the stripped H<sup>+</sup> beam with a power of about 5W equivalent was expected even if the laser power of the present Nd:YAG laser system was set to the lower value of 5W.

## CONCLUSION

For the extraction of the low power H<sup>+</sup> beam (less than 10 W) from the high power H<sup>-</sup> beam (400 MeV, 250 kW) by the LCE technique, a preliminary LCE experiment to measure the power of the stripped H<sup>+</sup> beam was conducted using the H<sup>-</sup> beam with energy of 3 MeV from the RFQ linac in J-PARC. As a result of this experiment, the stripped H<sup>+</sup> beam with a power of about 5 W equivalent was obtained under the J-PARC linac beam condition, and this value almost satisfied the power requirement (less than 10 W) of the proton beam for the TEF-P.

In this experiment, we focused on the power of the stripped H<sup>+</sup> beam. We will conduct a further experiment to confirm the beam quality of the laser and the H<sup>-</sup>, as well as the long-term power stability of the stripped H<sup>+</sup> beam.

## REFERENCES

- [1] K. Tsujimoto *et al.*, “Feasibility of Lead-Bismuth-Cooled Accelerator-Driven System for Minor-Actinide Transmutation”, *Nucl. Tech.*, vol. 161, pp. 315-328, 2008.
- [2] H. Oigawa *et al.*, “Conceptual Design of Transmutation Experimental Facility”, in *Proc. Global2001*, Paris, France (CD-ROM, 2001).
- [3] Y. Liu *et al.*, “Laser wire beam profile monitor in the spallation neutron source (SNS) superconducting linac”, *Nucl. Instr. Meth.*, vol. A612, pp. 241-253, 2010.
- [4] S. Meigo *et al.*, “A Feasibility Study of H<sup>-</sup> Beam Extraction Technique Using YAG Laser”, JAERI, Tokai, Ibaraki, JAPAN, Rep. JAERI-Tech 2002-095, Dec. 2002, (in Japanese).
- [5] John T. Broad and William P. Reinhardt, “One- and two-electron photoejection from H<sup>-</sup>: A multichannel J-matrix calculation”, *Phys. Rev.*, vol. A14, pp. 2159-2173, 1976.
- [6] K. Hirano *et al.*, “Development of beam scrapers using a 3-MeV linac at J-PARC”, in *Proc. 13th Annual Meeting of Particle Accelerator Society of Japan*, Chiba, Aug. 2016, paper MOP005, (in Japanese).